

# Narrow escape to small windows on a small ball modeling the viral entry into the cell nucleus

T. Lagache<sup>1,2</sup> and D. Holcman<sup>1,3</sup> \*

December 7, 2021

## Abstract

A certain class of viruses replicates inside a cell if they can enter the nucleus through one of many small target pores, before being permanently trapped or degraded. We adopt for viral motion a switching stochastic process model and we estimate here the probability and the conditional mean first passage time for a viral particle to attain alive the nucleus. The cell nucleus is covered with thousands of small absorbing nuclear pores and the minimum distance between them defines the smallest spatial scale that limits the efficiency of stochastic simulations. Using the Neuman-Green's function method to solve the steady-state Fokker-Planck equation, we derive asymptotic formula for the probability and mean arrival time to a small window for various pores' distributions, that agree with stochastic simulations. These formulas reveal how key geometrical parameters defines the cytoplasmic stage of viral infection.

## 1 Introduction

How particles such as molecules, proteins, DNA, RNA, or viruses are moving inside the complex and crowded cellular environment [18] remains a challenge both experimentally and theoretically. For example, vesicles or RNA granules [8] have to reach small targets in order to deliver their payload or trigger protein synthesis. However, large DNA or plasmid are too large and cannot pass the cytoplasmic crowded organization [7]. In some cases, large particles are transported intermittently along microtubules (MTs) toward

---

<sup>\*1</sup> Applied Mathematics and Computational Biology, Ecole Normale Supérieure, France. <sup>2</sup> The NeuroTechnology Center at Columbia University Biological Sciences 901 NWC Building, 550 West 120th Street, New York, N.Y. 10027. [tl2756@columbia.edu](mailto:tl2756@columbia.edu). <sup>3</sup> Newton Institute, Churchill college and DAMTP Cambridge CB30DS, United Kingdom.

the nucleus and Brownian motion inside the cytoplasm. Many viruses containing DNA have the ability to hijack the cellular transport machinery to reach a nuclear pore and deliver their genetic material inside the nucleus [24, 9]. Although viral trajectories can be monitored *in vivo* using live microscopy, for viruses such as HIV or the Adeno-Associated Virus [1, 22], these trajectories consist of alternating epochs of diffusion and directed motion. The precise nature of these trajectories remains unclear. In addition, on their way to the nucleus, viruses can be trapped in the cytoplasm or degraded through several pathways (including the ubiquitin-proteasome).

To quantify the success of the early steps of viral infection, we recently used a modeling approach at the single particle level [10, 13]. Due to small size of the nuclear pore (Fig. 1), Brownian simulations are always ineffective to estimate precisely the moments associated to arrival time. To study the dependency with respect to geometrical and dynamical parameters, we analyzed the intermittent stochastic dynamics of viruses along MTs and derive asymptotic formula for the conditional mean first passage time (MFPT)  $\tau_n$  and the probability  $P_n$  that a single particle arrives to  $n$  small targets [10, 15]. However, our previous formula are valid when the number of absorbing holes (targets) is not too large. We extend here our analysis to the case of many holes. This analysis relies on the explicit expansion of the Neumann-Green's function to order three [19]. The present method is also valid for many interacting small holes [21, 12, 4].

The paper is organized as follows. We first recall our previous model of viral particles and the stochastic description of trajectories. Second, we extend the small hole interaction method to the case of a stochastic particle with a drift and derive the mean arrival time using an interaction matrix between holes. Using the precise expansion of the Neumann-Green's function for the sphere, we will derive new asymptotic formula for the probability and the mean conditioning time to reach one of the many nuclear pore. Finally, we confirm our analysis with some Brownian simulations. The new formula that significantly improve our previous effort [10, 15] can now be used to study more precisely the first steps of viral infection in cells.

## 2 The mean time to a small nuclear pore.

Intermittent trajectories of a viral particle  $\mathbf{x}(t)$  were described by the switching stochastic rule [14]

$$d\mathbf{x} = \begin{cases} \sqrt{2D}d\mathbf{w} & \text{when } \mathbf{x}(t) \text{ is free} \\ \mathbf{V}dt & \mathbf{x}(t) \text{ bound,} \end{cases} \quad (1)$$

where  $\mathbf{w}$  is a standard 3d-Brownian motion,  $D$  the diffusion constant and  $\mathbf{V}$  the velocity of the directed motion along MTs (randomly distributed). The switching dynamics depends

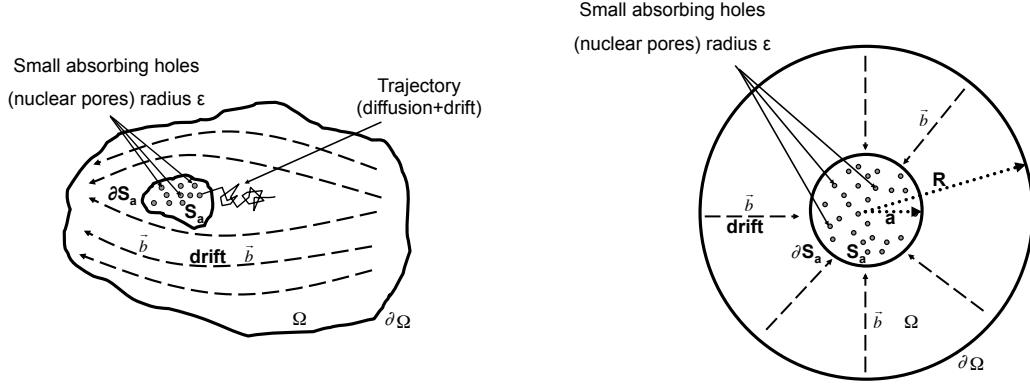


Figure 1: **Schematic representation of the cell cytoplasm as a 3-dimensional domain  $\Omega$ .** (Right-hand side): Stochastic trajectories, solutions of eq. 2, that contains both a diffusion and a drift terms can be absorbed at small windows with radius  $\epsilon \ll |\Omega|^{1/3}$  located on the surface of the nucleus  $\partial S_a$ . Right-hand side: simplified spherical cell (radius  $R$ ) containing a spherical nucleus that we model with a ball of radius  $a$  such that  $\epsilon \ll a \ll |\Omega|^{1/3}$ .

on the attachment and detachment rates [14]. We coarse-grained this switching process into by a steady-state stochastic equation

$$d\mathbf{x} = \mathbf{b}(\mathbf{x})dt + \sqrt{2D}d\mathbf{w}, \quad (2)$$

where the effective drift  $\mathbf{b}(\mathbf{x})$  was found using the following criteria: inside the cytoplasm  $\Omega$ , the mean first passage time of stochastic processes 1 and 2 is the same [14, 15]. The drift  $\mathbf{b}(\mathbf{x})$  depends on the cell geometry, the number and distribution of MTs and the rates of binding and unbinding of the particle to MTs.

Most viruses have to reach one of the small circular pore, modeled as absorbing windows of radius  $\epsilon \ll 1$  located on the boundary  $\partial S_a$  of the nucleus. We approximate a small pore as a small sphere  $S_a$ . The external cell membrane defines the boundary  $\partial\Omega$  for the stochastic process eq. 2. The cell cytoplasm is represented as the three-dimensional bounded domain  $\Omega$ , whose boundary is  $\partial\Omega \cup \partial S_a$ . It consists of a reflecting part except for the  $n$ -small absorbing windows  $\partial N_a$  located on the nucleus (fig.1-left).

Finally, we model the degradation activity in the cytoplasm by a steady-state killing rate  $k(\mathbf{x})$  and a trajectory described by eq. 2 can thus disappear before reaching the absorbing boundary  $\partial N_a$ . The survival probability density function (SPDF) is solution of the forward Fokker-Planck equation [11]

$$\begin{aligned} \frac{\partial p}{\partial t} &= \Delta p - \nabla \cdot \mathbf{b}p - kp \\ p(\mathbf{x}, 0) &= p_i(\mathbf{x}) \end{aligned} \quad (3)$$

with the boundary conditions:

$$p(\mathbf{x}, t) = 0 \text{ on } \partial N_a \text{ and } \mathbf{J}(\mathbf{x}, t) \cdot \mathbf{n}_x = 0 \text{ on } \partial\Omega \cup (\partial S_a - \partial N_a) \quad (4)$$

where the flux density vector is

$$\mathbf{J}(\mathbf{x}, t) = -D\nabla p(\mathbf{x}, t) + \mathbf{b}(\mathbf{x})p(\mathbf{x}, t). \quad (5)$$

where  $\mathbf{n}_x$  is the normal derivative at a point  $\mathbf{x}$ .

We recall that the mean probability  $\langle P \rangle$  and the conditional MFPT  $\langle \tau \rangle$  (averaged over the initial particle distribution) for a stochastic particle driven by eq. 2 to reach the boundary  $\partial N_a$  before degradation can be expressed using  $\tilde{p}(\mathbf{x}) = \int_0^\infty p(\mathbf{x}, t) dt$  and  $q(\mathbf{x}) = \int_0^\infty tp(\mathbf{x}, t) dt$  [10] as

$$\langle P \rangle(n, \epsilon) = 1 - \int_{\Omega} k(\mathbf{x})\tilde{p}(\mathbf{x})d\mathbf{x}, \quad (6)$$

and

$$\langle \tau \rangle(n, \epsilon) = \frac{\int_{\Omega} \tilde{p}(\mathbf{x})d\mathbf{x} - \int_{\Omega} k(\mathbf{x})q(\mathbf{x})d\mathbf{x}}{1 - \int_{\Omega} k(\mathbf{x})\tilde{p}(\mathbf{x})d\mathbf{x}}. \quad (7)$$

For a potential drift  $\mathbf{b}(\mathbf{x}) = -\nabla\Phi(\mathbf{x})$ , an asymptotic expansion in the small parameter  $\epsilon$  [15], reveals that

$$\left\{ \begin{array}{l} \langle P \rangle(n, \epsilon) = \frac{e^{-\frac{\Phi_0}{D}}}{\frac{1}{4Dn\epsilon} \int_{\Omega} e^{-\frac{\Phi(\mathbf{x})}{D}} k(\mathbf{x})d\mathbf{x} + e^{-\frac{\Phi_0}{D}}} \\ \langle \tau \rangle(n, \epsilon) = \frac{\frac{1}{4Dn\epsilon} \int_{\Omega} e^{-\frac{\Phi(\mathbf{x})}{D}} d\mathbf{x}}{\frac{1}{4Dn\epsilon} \int_{\Omega} e^{-\frac{\Phi(\mathbf{x})}{D}} k(\mathbf{x})d\mathbf{x} + e^{-\frac{\Phi_0}{D}}}, \end{array} \right. \quad (8)$$

where  $\Phi_0$  is the constant value of the radial potential  $\Phi(\mathbf{x})$  on the centered nucleus where the nuclear pores are uniformly distributed. The range of validity of these asymptotic expressions has been explored with Brownian simulations for a single hole [13]. However, these formulas do not account for the possible interactions between the small absorbing pores, and for a large number of nuclear pores  $n \gg 1$ ,

$$\lim_{n \rightarrow \infty, n\epsilon^2 \ll 1} \langle \tau \rangle(n, \epsilon) = 0, \quad (9)$$

which shows the limitation of the previous formula.

We find here the correction term that accounts for the nuclear geometry. Interactions between absorbing windows can drastically affect the MFPT [12, 6], and we study here these interactions and extend the narrow escape time for a stochastic particle (with a drift) in the presence of a killing field  $k(\mathbf{x})$  to reach one of the interacting absorbing windows located on the nucleus. We obtain an estimate for the probability  $\langle P \rangle$  and the associated conditional MFPT  $\langle \tau \rangle$ . Both quantities are solutions of a coupled system of partial differential equations. For a large number of holes covering homogeneously the nucleus, we extend our analysis using a mean field approximation and obtain formulas for the probability  $\langle P \rangle$  and the mean time  $\langle \tau \rangle$ , valid for a large range of both parameters  $\epsilon$  and  $n$ , generalizing formula 8. Finally, we test the asymptotical results against Brownian simulations and apply our formula to model viral trafficking ( $\mathbf{b} \neq \mathbf{0}$ ) and non-viral gene vectors (Brownian diffusion  $\mathbf{b} = \mathbf{0}$ ) that have to reach one of the  $n \approx 2,000 \gg 1$  [17] nuclear pores covering the nucleus in order to deliver their genetic material inside the cell nucleus.

### 3 Asymptotic derivations of the mean time $\langle \tau \rangle$ and the probability $\langle P \rangle$

The  $n$ -absorbing windows  $\partial N_a = \bigcup_{i=1}^n \partial \Omega_i$  have the same radius  $\epsilon$ , centered at positions  $(\mathbf{x}_i)_{i=1}^n$ . The steady state SPDF  $p$  is solution of eq. 3) [11].

The Neumann-Green function  $\mathcal{N}(\mathbf{x}, \mathbf{x}_0)$  is solution of the differential equation [10]

$$\begin{aligned} \Delta \mathcal{N}(\mathbf{x}, \mathbf{x}_0) &= -\delta_{\mathbf{x}_0}(\mathbf{x}), \quad \mathbf{x} \in \Omega, \\ D \frac{\partial \mathcal{N}}{\partial n}(\mathbf{x}, \mathbf{x}_0) &= -\frac{1}{|\partial \Omega|} \quad \mathbf{x} \in \partial \Omega. \end{aligned} \quad (10)$$

We recall that  $\tilde{p}(\mathbf{x}) = \int_0^\infty p(\mathbf{x}, t) dt$  is solution of equation

$$\Delta \tilde{p} - \nabla \cdot (\mathbf{b} \tilde{p}) - k \tilde{p} = -p_i \quad (11)$$

with the boundary conditions

$$\tilde{p}(\mathbf{x}) = 0 \text{ on } \partial N_a = \bigcup_{i=1}^n \partial \Omega_i \text{ and } \tilde{\mathbf{J}}(\mathbf{x}) \cdot \mathbf{n}_x = 0 \text{ on } \partial \Omega \setminus (\partial S_a - \partial N_a) \quad (12)$$

where  $\tilde{\mathbf{J}}(\mathbf{x}) = -D \nabla \tilde{p}(\mathbf{x}) + \mathbf{b}(\mathbf{x}) \tilde{p}(\mathbf{x})$ .

Green's identity gives

$$\begin{aligned} I &= \int_{\Omega} (\Delta \tilde{p}(\mathbf{x}) - \nabla \cdot \mathbf{b} \tilde{p}(\mathbf{x}) - k \tilde{p}(\mathbf{x})) \mathcal{N}(\mathbf{x}, \mathbf{x}_0) d\mathbf{x} \\ &\quad - \int_{\Omega} \Delta \mathcal{N}(\mathbf{x}, \mathbf{x}_0) \tilde{p}(\mathbf{x}) d\mathbf{x}. \end{aligned} \quad (13)$$

Consequently, we have

$$I = - \int_{\Omega} p_i(\mathbf{x}) \mathcal{N}(\mathbf{x}, \mathbf{x}_0) + \tilde{p}(\mathbf{x}_0) \quad (14)$$

and from Green's identity

$$\begin{aligned} I &= - \int_{\partial N_a} \tilde{\mathbf{J}}(\mathbf{x}) \cdot \mathbf{n}_x \mathcal{N}(\mathbf{x}, \mathbf{x}_0) d\mathbf{x} + \int_{\Omega} \mathbf{b}(\mathbf{x}) \cdot \nabla \mathcal{N}(\mathbf{x}, \mathbf{x}_0) \tilde{p}(\mathbf{x}) d\mathbf{x} \\ &\quad - \int_{\Omega} k(\mathbf{x}) \tilde{p}(\mathbf{x}) d\mathbf{x} + \frac{1}{|\partial\Omega|} \int_{\partial\Omega} \tilde{p}(\mathbf{x}) d\mathbf{x}. \end{aligned} \quad (15)$$

Thus, we obtain

$$\begin{aligned} \int_{\Omega} (k(\mathbf{x}) \tilde{p} - p_i(\mathbf{x})) \mathcal{N}(\mathbf{x}, \mathbf{x}_0) d\mathbf{x} &= - \int_{\partial N_a} \tilde{\mathbf{J}}(\mathbf{x}) \cdot \mathbf{n}_x \mathcal{N}(\mathbf{x}, \mathbf{x}_0) d\mathbf{x} \\ &\quad + \int_{\Omega} \mathbf{b}(\mathbf{x}) \cdot \nabla \mathcal{N}(\mathbf{x}, \mathbf{x}_0) \tilde{p}(\mathbf{x}) d\mathbf{x} \\ &\quad + \frac{1}{|\partial\Omega|} \int_{\partial\Omega} \tilde{p}(\mathbf{x}) d\mathbf{x} - \tilde{p}(\mathbf{x}_0). \end{aligned} \quad (16)$$

When the field is the gradient of a potential and when the first eigenvalue only contribute to the spectrum, the solution  $\tilde{p}(\mathbf{x})$  is the steady-state, thus:

$$\tilde{p}(\mathbf{x}) \approx C_{\epsilon} e^{-\frac{\Phi(\mathbf{x})}{D}} + O(1). \quad (17)$$

Furthermore,

$$q(\mathbf{x}) = \left( C_{\epsilon}^2 \int_{\Omega} e^{-\frac{\phi(\mathbf{x})}{D}} d\mathbf{x} \right) e^{-\frac{\Phi(\mathbf{x})}{D}} + O(1), \quad (18)$$

For a smooth initial distributions  $p_i$ , the integral

$$\int_{\Omega} p_i(\mathbf{x}) \mathcal{N}(\mathbf{x}, \mathbf{x}_i) d\mathbf{x} \quad (19)$$

is uniformly bounded as  $\epsilon \rightarrow 0$ , while all other terms in relation 16 are unbounded. Consequently, for a small degradation rate  $k \ll 1$  limit, the integral equation (16) is to leading order:

$$\begin{aligned} \tilde{p}(\mathbf{x}_0) + O(1) &= - \int_{\partial N_a} \tilde{\mathbf{J}}(\mathbf{x}) \cdot \mathbf{n}_x \mathcal{N}(\mathbf{x}, \mathbf{x}_0) d\mathbf{x} + \int_{\Omega} \mathbf{b}(\mathbf{x}) \cdot \nabla \mathcal{N}(\mathbf{x}, \mathbf{x}_0) \tilde{p}(\mathbf{x}) d\mathbf{x} \\ &\quad + \frac{1}{|\partial\Omega|} \int_{\partial\Omega} \tilde{p}(\mathbf{x}) d\mathbf{x}. \end{aligned} \quad (20)$$

For  $\mathbf{x}_0$  at a distance  $O(1)$  away from absorbing windows,  $\mathcal{N}(\mathbf{x}, \mathbf{x}_0)$  is uniformly bounded for  $\mathbf{x} \in \partial\Omega_a$ . In addition, integrating (11) over  $\Omega$  we obtain:

$$\int_{\partial N_a} \tilde{\mathbf{J}}(\mathbf{x}) \cdot \mathbf{n}_x d\mathbf{x} = 1 - \int_{\Omega} k(\mathbf{x}) \tilde{p}(\mathbf{x}) d\mathbf{x} = \langle P \rangle \in [0, 1]. \quad (21)$$

Consequently, for  $\mathbf{x}_0$  at a distance  $O(1)$  away from absorbing windows,  $\int_{\partial N_a} \tilde{\mathbf{J}}(\mathbf{x}) \cdot \mathbf{n}_x \mathcal{N}(\mathbf{x}, \mathbf{x}_0) d\mathbf{x}$  is uniformly bounded, and

$$\frac{1}{|\partial\Omega|} \int_{\partial\Omega} \tilde{p}(\mathbf{x}) d\mathbf{x} + \int_{\Omega} \mathbf{b}(\mathbf{x}) \cdot \nabla \mathcal{N}(\mathbf{x}, \mathbf{x}_0) \tilde{p}(\mathbf{x}) d\mathbf{x} = C_\epsilon e^{-\frac{\Phi(\mathbf{x}_0)}{D}} + O(1). \quad (22)$$

Consequently, (20) reduces to

$$\tilde{p}(\mathbf{x}_0) + O(1) = - \int_{\partial N_a} \tilde{\mathbf{J}}(\mathbf{x}) \cdot \mathbf{n}_x \mathcal{N}(\mathbf{x}, \mathbf{x}_0) d\mathbf{x} + C_\epsilon e^{-\frac{\Phi(\mathbf{x}_0)}{D}} \quad (23)$$

We now compute  $\int_{\partial N_a} \tilde{\mathbf{J}}(\mathbf{x}) \cdot \mathbf{n}_x \mathcal{N}(\mathbf{x}, \mathbf{x}_0) d\mathbf{x} = \sum_{i=1}^n \int_{\partial\Omega_i} \tilde{\mathbf{J}}(\mathbf{x}) \cdot \mathbf{n}_x \mathcal{N}(\mathbf{x}, \mathbf{x}_0) d\mathbf{x}$ , by decomposing the flux

$$\left( \tilde{\mathbf{J}}(\mathbf{x}) \cdot \mathbf{n}_x \right)_{\mathbf{x} \in \partial\Omega_i} = g_i(\mathbf{x}) + f_i(\mathbf{x}), \quad (24)$$

where the leading order  $g_i(s)$  with

$$s = |\mathbf{x} - \mathbf{x}_i| \quad (25)$$

into

$$g_i(s) = \frac{g_0^i}{\sqrt{\epsilon^2 - s^2}}, \quad (26)$$

and  $g_0^i$  a constant and  $f_i$  is a regular function such that

$$\int_0^\epsilon f_i(s) ds = O(\epsilon g_0^i). \quad (27)$$

Choosing  $\mathbf{x}_0 = \mathbf{x}_i$  at the absorbing boundary condition, we get that  $\tilde{p}(\mathbf{x}_i) = 0$ . For  $i \neq j$ , and  $|\mathbf{x}_i - \mathbf{x}_j| \gg \epsilon$  and that for  $\mathbf{x} \in \partial\Omega_j$ ,

$$\mathcal{N}(\mathbf{x}, \mathbf{x}_i) = \mathcal{N}(\mathbf{x}_j, \mathbf{x}_i) + O(\epsilon). \quad (28)$$

Consequently, using the flux expansion 24, we get

$$\int_{\partial N_a} \tilde{\mathbf{J}}(\mathbf{x}) \cdot \mathbf{n}_x \mathcal{N}(\mathbf{x}, \mathbf{x}_i) d\mathbf{x} = \int_{\partial\Omega_i} (g_i(\mathbf{x}) + f_i(\mathbf{x})) \mathcal{N}(\mathbf{x}, \mathbf{x}_i) d\mathbf{x} \quad (29)$$

$$+ \sum_{j=1, j \neq i}^n (\mathcal{N}(\mathbf{x}_j, \mathbf{x}_i) + O(\epsilon)) \int_{\partial\Omega_j} (g_j(\mathbf{x}) + f_j(\mathbf{x})) d\mathbf{x}. \quad (30)$$

For  $\mathbf{x}_i$  on the domain boundary  $\partial S_a$ , the Neumann-Green's function  $\mathcal{N}(\mathbf{x}, \mathbf{x}_i)$  can be written as [23]:

$$\mathcal{N}(\mathbf{x}, \mathbf{x}_i) = \frac{1}{2\pi D |\mathbf{x} - \mathbf{x}_i|} + \frac{L(\mathbf{x}_i) + N(\mathbf{x}_i)}{8\pi D} \log \left( \frac{1}{|\mathbf{x} - \mathbf{x}_i|} \right) + \omega_{\mathbf{x}_i}(\mathbf{x}), \quad (31)$$

where  $L(\mathbf{x}_i)$  and  $N(\mathbf{x}_i)$  are the principal curvatures of  $\partial S_a$  at  $\mathbf{x}_i$  and  $\omega_{\mathbf{x}_i}(\mathbf{x})$  is the regular part of the Green function, which is bounded for  $\mathbf{x}$  in  $\Omega$ .

However, when the absorbing small patches are located on the boundary of a small ball of radius  $a$ , The Green-Neumann's expansion 31 of  $\mathcal{N}(\mathbf{x}_i, \mathbf{x}_j)$  does not hold, because the second term  $\frac{-1}{4\pi a D} \log\left(\frac{1}{|\mathbf{x}_i - \mathbf{x}_j|}\right)$  can become much larger than the first term  $\frac{1}{2\pi D |\mathbf{x}_i - \mathbf{x}_j|}$  when  $|\mathbf{x}_i - \mathbf{x}_j| \approx a$ , and  $a \ll |\Omega|^{\frac{1}{3}}$ .

### 3.1 Analysis for a small internal ball

We start with the revisited solution of the Neumann's equation

$$\begin{aligned} D\Delta\tilde{\mathcal{N}}(\mathbf{x}, \mathbf{x}_0) &= -\delta(\mathbf{x} - \mathbf{x}_0), \text{ for } \mathbf{x} \in \mathbb{R}^3 \\ D\frac{\partial\tilde{\mathcal{N}}}{\partial n}(\mathbf{x}, \mathbf{x}_0) &= 0, \text{ for } \mathbf{x} \in S_a. \end{aligned} \quad (32)$$

which is equal for  $|\mathbf{x}_0| = |\mathbf{x}| = a$  to (see appendix)

$$\tilde{\mathcal{N}}(\mathbf{x}, \mathbf{x}_0) = \frac{1}{2\pi D |\mathbf{x} - \mathbf{x}_0|} + \frac{1}{4\pi a D} \log\left(\frac{|\mathbf{x} - \mathbf{x}_0|}{2a + |\mathbf{x} - \mathbf{x}_0|}\right). \quad (33)$$

Thus for  $\mathbf{x}$  and  $\mathbf{x}_0$  in the neighborhood of the sphere  $S_a$ , we have

$$\mathcal{N}(\mathbf{x}, \mathbf{x}_0) = \tilde{\mathcal{N}}(\mathbf{x}, \mathbf{x}_0) + O(1). \quad (34)$$

Consequently, using the geodesic distance  $s = d(P, \mathbf{x}_i)$ , expanding the flux term in relation 29 gives

$$\begin{aligned} \int_{\partial N_a} \tilde{\mathbf{J}}(\mathbf{x}) \cdot \mathbf{n}_x \mathcal{N}(\mathbf{x}, \mathbf{x}_i) d\mathbf{x} &= \int_0^\epsilon \left( \frac{g_0^i}{\sqrt{\epsilon^2 - s^2}} + f_i(s) \right) \\ &\quad \left( \frac{1}{2\pi D s} + \frac{1}{4\pi a D} \log\left(\frac{s}{2a + s}\right) + O(1) \right) 2\pi s ds \\ &\quad + \sum_{j=1, j \neq i}^n (\mathcal{N}(\mathbf{x}_j, \mathbf{x}_i) + 0(\epsilon)) \int_0^\epsilon \left( \frac{g_0^j}{\sqrt{\epsilon^2 - s^2}} + f_j(s) \right) 2\pi s ds. \end{aligned} \quad (35)$$

Using condition (27), we obtain:

$$\begin{aligned} \int_{\partial N_a} \tilde{\mathbf{J}}(\mathbf{x}) \cdot \mathbf{n}_x \mathcal{N}(\mathbf{x}, \mathbf{x}_0) d\mathbf{x} &= \frac{g_0^i}{D} \left( \frac{\pi}{2} + \frac{\epsilon}{2a} \log\left(\frac{\epsilon}{a}\right) + O(\epsilon) \right) \\ &\quad + 2\pi\epsilon \sum_{j=1, j \neq i}^n \mathcal{N}(\mathbf{x}_j, \mathbf{x}_i) g_0^j (1 + O(\epsilon)). \end{aligned} \quad (36)$$



We recall that the constant  $g_0^i$  is of order  $g_0^i = O\left(\frac{1}{n\epsilon}\right)$ , and that

$$\mathcal{N}(\mathbf{x}_j, \mathbf{x}_i) = O\left(\frac{1}{|\mathbf{x}_i - \mathbf{x}_j|}\right) = O\left(\frac{1}{a}\right), \quad (37)$$

thus we rewrite the flux condition as

$$\begin{aligned} \int_{\partial N_a} \tilde{\mathbf{J}}(\mathbf{x}) \cdot \mathbf{n}_x \mathcal{N}(\mathbf{x}, \mathbf{x}_0) d\mathbf{x} &= \frac{g_0^i}{D} \left( \frac{\pi}{2} + \frac{\epsilon}{2a} \log\left(\frac{\epsilon}{a}\right) \right) \\ &+ 2\pi\epsilon \sum_{j=1, j \neq i}^n \mathcal{N}(\mathbf{x}_j, \mathbf{x}_i) g_0^j + O\left(\frac{\epsilon}{a}\right) + O\left(\frac{1}{n}\right). \end{aligned} \quad (38)$$

Injecting 39 in 23, for  $\mathbf{x}_0 = \mathbf{x}_i$ , we obtain the system of  $n$  equations to solve in the  $n+1$  variable  $(g_0^1, \dots, g_0^n, C_\epsilon)$ :

$$\left( \frac{\pi}{2D} + \frac{\epsilon}{2aD} \log\left(\frac{\epsilon}{a}\right) \right) g_0^i + 2\pi\epsilon \sum_{j=1, j \neq i}^n \mathcal{N}(\mathbf{x}_j, \mathbf{x}_i) g_0^j = C_\epsilon e^{-\frac{\Phi(\mathbf{x}_i)}{D}} + O(1). \quad (39)$$

To close the system of equation, we use the compatibility condition (eq. 21) with expression 24 and approximation 17 for the function  $\tilde{p}$ :

$$2\pi\epsilon \sum_{i=1}^n g_0^i = 1 - C_\epsilon \int_{\Omega} k(\mathbf{x}) e^{-\frac{\Phi(\mathbf{x})}{D}} d\mathbf{x} + O(1), \quad (40)$$

Finally, we obtain a linear system of  $n+1$  equations (39) and (40) for the flux constant  $g_0^i$  ( $i \leq i \leq n$ ), and for the parameter  $C_\epsilon$ , summarized as

$$\begin{cases} \frac{\pi}{2D} + \frac{\epsilon}{2aD} \log\left(\frac{\epsilon}{a}\right) g_0^i + 2\pi\epsilon \sum_{j=1, j \neq i}^n \mathcal{N}(\mathbf{x}_j, \mathbf{x}_i) g_0^j = C_\epsilon e^{-\frac{\Phi(\mathbf{x}_i)}{D}} + O(1), \text{ for } 1 \leq i \leq n \\ 2\pi\epsilon \sum_{i=1}^n g_0^i = 1 - C_\epsilon \int_{\Omega} k(\mathbf{x}) e^{-\frac{\Phi(\mathbf{x})}{D}} d\mathbf{x} + O(1) \end{cases} \quad (41)$$

We will now obtain asymptotic estimates for  $C_\epsilon$ ,  $\langle P \rangle$  and  $\langle \tau \rangle$ , by solving the linear system of equations 41 in the limit  $\epsilon$  small. Injecting expressions 17 and 18 for  $\tilde{p}(\mathbf{x})$  and  $q(\mathbf{x})$  in 6-7, we obtain

$$\langle P \rangle = 1 - C_\epsilon \int_{\Omega} k(\mathbf{x}) e^{-\frac{\Phi(\mathbf{x})}{D}} d\mathbf{x} \text{ and } \langle \tau \rangle = C_\epsilon \int_{\Omega} e^{-\frac{\Phi(\mathbf{x})}{D}} d\mathbf{x}. \quad (42)$$

We derive the asymptotic expression in the next section.

## 4 Mean field approximation and asymptotics formula for $\langle \tau \rangle$ and $\langle P \rangle$ for $n \gg \frac{1}{\epsilon}$

We derive now expressions for  $\langle P \rangle$  and  $\langle \tau \rangle$  in the limit  $n \gg 1$  and absorbing windows are distributed with a density  $\rho(\mathbf{x})$  over the spherical nucleus  $S_a$ . By summing equations eq. 39 for  $1 \leq i \leq n$ , we obtain that

$$\left( \frac{\pi}{2D} + \frac{\epsilon}{2aD} \log \left( \frac{\epsilon}{a} \right) \right) \sum_{i=1}^n g_0^i + 2\pi\epsilon \sum_{i=1}^n g_0^i \sum_{j=1, j \neq i}^n \mathcal{N}(\mathbf{x}_j, \mathbf{x}_i) = C_\epsilon \sum_{i=1}^n e^{-\frac{\Phi(\mathbf{x}_i)}{D}} + O(n). \quad (43)$$

When  $\mathbf{x}_i$  is located at the north pole, the distance  $|\mathbf{x}_i - \mathbf{x}_j|$  with  $j^{th}$  located at position  $\mathbf{x}_j(\theta, \phi)$  is given by  $|\mathbf{x}_i - \mathbf{x}_j| = 2a \sin \left( \frac{\phi}{2} \right)$  and the Neumann function is

$$\tilde{\mathcal{N}}(\mathbf{x}_j(\theta, \phi), \mathbf{x}_i) = \frac{1}{4\pi a D} \left( \frac{1}{\sin \left( \frac{\phi}{2} \right)} + \log \left( \frac{\sin \left( \frac{\phi}{2} \right)}{1 + \sin \left( \frac{\phi}{2} \right)} \right) \right). \quad (44)$$

We use now that the probability density function  $\rho_i(\phi)$  of the  $j \neq i$  windows (north pole  $i$ ) is normalized by the condition

$$\int_0^\pi 2\pi a^2 \rho_i(\phi) \sin(\phi) d\phi = 1, \quad (45)$$

thus

$$\begin{aligned} \lim_{n \rightarrow \infty} \frac{1}{n} \sum_{j=1, j \neq i}^n \mathcal{N}(\mathbf{x}_j, \mathbf{x}_i) &= \int_0^\pi \frac{1}{4\pi a D} \left( \frac{1}{\sin \left( \frac{\phi}{2} \right)} + \log \left( \frac{\sin \left( \frac{\phi}{2} \right)}{1 + \sin \left( \frac{\phi}{2} \right)} \right) \right) \rho_i(\phi) 2\pi a^2 \sin(\phi) d\phi \\ &= \frac{a}{2D} \int_0^\pi \left( \frac{1}{\sin \left( \frac{\phi}{2} \right)} + \log \left( \frac{\sin \left( \frac{\phi}{2} \right)}{1 + \sin \left( \frac{\phi}{2} \right)} \right) \right) \rho_i(\phi) \sin(\phi) d\phi. \end{aligned} \quad (46)$$

In addition, we can also approximate

$$\lim_{n \rightarrow \infty} \frac{1}{n} \sum_{i=1}^n e^{-\frac{\Phi(\mathbf{x}_i)}{D}} = a^2 \int_0^{2\pi} \int_0^\pi e^{-\frac{\Phi(\phi, \theta)}{D}} \rho(\phi) d\phi d\theta, \quad (47)$$

We now re-write relation 43 using

$$I_1^i = \int_0^\pi \left( \frac{1}{\sin \left( \frac{\phi}{2} \right)} + \log \left( \frac{\sin \left( \frac{\phi}{2} \right)}{1 + \sin \left( \frac{\phi}{2} \right)} \right) \right) \rho_i(\phi) \sin(\phi) d\phi, \quad (48)$$

$$I_2 = \int_0^{2\pi} \int_0^\pi e^{-\frac{\Phi(\phi, \theta)}{D}} \rho(\phi, \theta) \sin(\phi) d\phi d\theta, \quad (49)$$

so that

$$\left(\frac{\pi}{2D} + \frac{\epsilon}{2aD} \log\left(\frac{\epsilon}{a}\right)\right) \sum_{i=1}^n g_0^i + \frac{na\pi\epsilon}{D} \sum_{i=1}^n g_0^i I_1^i = C_\epsilon na^2 I_2 + O(n). \quad (50)$$

For identically distributed windows  $I_1^i = I_1$  with  $1 \leq i \leq n$ . Using the compatibility condition 40 in equation 50, we obtain

$$\left(\frac{1}{4D\epsilon} + \frac{1}{4\pi aD} \log\left(\frac{\epsilon}{a}\right) + \frac{na}{2D} I_1\right) \left(1 - C_\epsilon \int_{\Omega} k(\mathbf{x}) e^{-\frac{\Phi(\mathbf{x})}{D}} d\mathbf{x}\right) = C_\epsilon na^2 I_2 + O(n). \quad (51)$$

Thus we obtain to leading order

$$C_\epsilon = \frac{\pi a + \epsilon \log\left(\frac{\epsilon}{a}\right) + 2n\pi a^2 \epsilon I_1}{\left(\pi a + \epsilon \log\left(\frac{\epsilon}{a}\right) + 2n\pi a^2 \epsilon I_1\right) \int_{\Omega} k(\mathbf{x}) e^{-\frac{\Phi(\mathbf{x})}{D}} d\mathbf{x} + 4\pi na^3 D \epsilon I_2} \quad (52)$$

To further compute for the probability  $\langle P \rangle$  and the MFPT  $\langle \tau \rangle$  using expression 52, we shall consider two distributions of windows:

1. Random distribution
2. Uniform distribution

## 4.1 Random distribution of narrow windows located on a sphere

When there  $n \gg 1$  non-overlapping windows randomly distributed on the sphere, the probability distribution of windows is given by

$$\rho(\phi, \theta) = \rho_i(\phi) = \frac{1}{4\pi a^2} \mathbf{1}_{\{\phi > 2 \arcsin(\frac{\epsilon}{a})\}}, \quad (53)$$

for all  $1 \leq i \leq n$ . The condition  $\{\phi > 2 \arcsin(\frac{\epsilon}{a})\}$  ensures non-overlapping. Changing the variable  $y = \sin\left(\frac{\phi}{2}\right)$ , we re-write

$$I_1 = \frac{1}{\pi a^2} \int_{\frac{\epsilon}{a}}^1 \left(\frac{1}{y} + \log\left(\frac{y}{1+y}\right)\right) y dy = \frac{1}{2\pi a^2} \left[ x + \log(1+x) + x^2 \log\left(\frac{x}{1+x}\right) \right]_{\frac{\epsilon}{a}}^1, \quad (54)$$

that is

$$I_1 = \frac{1}{2\pi a^2} \left(1 - 2\frac{\epsilon}{a} - \frac{\epsilon^2}{a^2} \log\left(\frac{\epsilon}{a}\right)\right). \quad (55)$$

In addition, we have

$$I_2 = \frac{1}{4\pi a^2} \int_0^{2\pi} \int_{2 \arcsin(\frac{\epsilon}{a})}^{\pi} e^{-\frac{\Phi(\phi, \theta)}{D}} \sin(\phi) d\phi d\theta. \quad (56)$$

Replacing in eq. 52,  $I_1$  and  $I_2$  by expressions 55 and 56, we obtain to leading order for randomly distributed windows,

$$C_\epsilon^{\text{rand}} = \frac{1}{\int_{\Omega} k(\mathbf{x}) e^{-\frac{\Phi(\mathbf{x})}{D}} d\mathbf{x} + C(n, \epsilon) \int_0^{2\pi} \int_{2\frac{\epsilon}{a}}^{\pi} e^{-\frac{\Phi(\phi, \theta)}{D}} \sin(\phi) d\phi d\theta}. \quad (57)$$

where

$$C(n, \epsilon) = \frac{naD\epsilon}{\pi a + \epsilon \left(1 - \frac{n\epsilon^2}{a^2}\right) \log\left(\frac{\epsilon}{a}\right) + n\epsilon \left(1 - 2\frac{\epsilon}{a}\right)}. \quad (58)$$

## 4.2 Homogeneous distribution of windows on the surface $S_a$

For small windows homogeneously distributed on a sphere, the density is given by [5]

$$\rho(\phi) = \mathbf{1}_{\{\phi > \arccos(1 - \frac{2}{n})\}} \frac{1}{4\pi a^2} \quad (59)$$

leading to

$$I_1 = \frac{1}{2\pi a^2} \left[ x + \log(1+x) + x^2 \log\left(\frac{x}{1+x}\right) \right]_{\frac{1}{2} \arccos(1 - \frac{2}{n})}^1, \quad (60)$$

and for  $n \gg 1$

$$I_1 = \frac{1}{2\pi a^2} \left( 1 - \frac{2}{\sqrt{n}} + \frac{\log(n)}{2n} \right) + o\left(\frac{\log(n)}{2n}\right). \quad (61)$$

In addition, we have

$$I_2 = \frac{1}{4\pi a^2} \int_0^{2\pi} \int_{2\arccos(1 - \frac{2}{n})}^{\pi} e^{-\frac{\Phi(\phi, \theta)}{D}} \sin(\phi) d\phi d\theta. \quad (62)$$

Replacing in equation 52,  $I_1$  and  $I_2$  by expressions 61 and 62 respectively, leads to

$$C_\epsilon^{\text{hom}} = \frac{1}{\int_{\Omega} k(\mathbf{x}) e^{-\frac{\Phi(\mathbf{x})}{D}} d\mathbf{x} + \tilde{C}_{\epsilon, n} \int_0^{2\pi} \int_{\frac{4}{\sqrt{n}}}^{\pi} e^{-\frac{\Phi(\phi, \theta)}{D}} \sin(\phi) d\phi d\theta}. \quad (63)$$

where

$$\tilde{C}_{\epsilon, n} = \frac{naD\epsilon}{\pi a + \epsilon \log\left(\frac{\sqrt{n}\epsilon}{a}\right) + n\epsilon \left(1 - \frac{2}{\sqrt{n}}\right)}. \quad (64)$$

Using formula 57 and 63 in expression 42, we obtain the asymptotic expressions for the probability and the condition MFPT that a stochastic particle reaches a small windows

$$\langle P \rangle = \frac{F(n, a, \epsilon) \int_0^{2\pi} \int_{\alpha_0}^{\pi} e^{-\frac{\Phi(\phi, \theta)}{D}} \sin(\phi) d\phi d\theta}{\int_{\Omega} k(\mathbf{x}) e^{-\frac{\Phi(\mathbf{x})}{D}} d\mathbf{x} + F(n, a, \epsilon) \int_0^{2\pi} \int_{\alpha_0}^{\pi} e^{-\frac{\Phi(\phi, \theta)}{D}} \sin(\phi) d\phi d\theta}, \quad (65)$$

and

$$\langle \tau \rangle = \frac{\int_{\Omega} e^{-\frac{\Phi(\mathbf{x})}{D}} d\mathbf{x}}{\int_{\Omega} k(\mathbf{x}) e^{-\frac{\Phi(\mathbf{x})}{D}} d\mathbf{x} + F(n, a, \epsilon) \int_0^{2\pi} \int_{\alpha_0}^{\pi} e^{-\frac{\Phi(\phi, \theta)}{D}} \sin(\phi) d\phi d\theta} \quad (66)$$

where

$$F(n, a, \epsilon) = \frac{naD\epsilon}{\left(\pi a + \epsilon \log\left(\frac{\epsilon}{a}\right) + n\epsilon(1 - 2\alpha_0 - \alpha_0^2 \log(\alpha_0))\right)} \quad (67)$$

and

$$\alpha_0 = \begin{cases} \frac{\epsilon}{a} & \text{for uniformly randomly distributed windows,} \\ \frac{1}{\sqrt{n}} & \text{for homogeneously distributed windows,} \end{cases} \quad (68)$$

When the drift is pointing towards the nucleus center and the potential  $\Phi(\mathbf{x}) = \Phi_0$  is constant at nuclear surface, then the probability and MFPT formulas reduce to

$$\langle P \rangle = \frac{4\pi F(n, a, \epsilon) e^{-\frac{\Phi_0}{D}}}{\int_{\Omega} k(\mathbf{x}) e^{-\frac{\Phi(\mathbf{x})}{D}} d\mathbf{x} + 4\pi F(n, a, \epsilon) e^{-\frac{\Phi_0}{D}}}, \quad (69)$$

and

$$\langle \tau \rangle = \frac{\int_{\Omega} e^{-\frac{\Phi(\mathbf{x})}{D}} d\mathbf{x}}{\int_{\Omega} k(\mathbf{x}) e^{-\frac{\Phi(\mathbf{x})}{D}} d\mathbf{x} + 4\pi F(n, a, \epsilon) e^{-\frac{\Phi_0}{D}}}. \quad (70)$$

When the drift  $\Phi_{S_a}$  restricted to  $S_a$  has a single global minima  $\Phi_m$  at position  $\mathbf{x}_0(\phi_0, \theta_0) \in S_a$ , we approximate integral  $I_2$  using Laplace's method. In the small diffusion limit  $D \ll \Phi(\mathbf{x})$  and large  $n$ , we get

$$I_2 = \frac{1}{4\pi a^2} \int_0^{2\pi} \int_{2\arccos(1-\frac{2}{n})}^{\pi} e^{-\frac{\Phi(\phi, \theta)}{D}} \sin(\phi) d\phi d\theta \approx \frac{D}{4a^2 \sqrt{\det[-H_{\Phi_{S_a}}(\mathbf{x}_0)]}} e^{-\frac{\Phi_m}{D}} \quad (71)$$

where  $\det[H_{\Phi_{S_a}}(\mathbf{x}_0)]$  is the determinant of the Hessian matrix of potential  $\Phi_{S_a}$  at  $\mathbf{x}_0$ . The probability and MFPT to a nuclear pore are then given by

$$\langle P \rangle = \frac{\pi D F(n, a, \epsilon) \sqrt{\det^{-1}[H_{\Phi_{S_a}}(\mathbf{x}_0)]} e^{-\frac{\Phi_m}{D}}}{\int_{\Omega} k(\mathbf{x}) e^{-\frac{\Phi(\mathbf{x})}{D}} d\mathbf{x} + \pi D F(n, a, \epsilon) \sqrt{\det^{-1}[H_{\Phi_{S_a}}(\mathbf{x}_0)]} e^{-\frac{\Phi_m}{D}}}, \quad (72)$$

and

$$\langle \tau \rangle = \frac{\int_{\Omega} e^{-\frac{\Phi(\mathbf{x})}{D}} d\mathbf{x}}{\int_{\Omega} k(\mathbf{x}) e^{-\frac{\Phi(\mathbf{x})}{D}} d\mathbf{x} + \pi D F(n, a, \epsilon) \sqrt{\det^{-1}[H_{\Phi_{S_a}}(\mathbf{x}_0)]} e^{-\frac{\Phi_m}{D}}} \quad (73)$$

A second Laplace's method can be used to estimate the volume integral. If the global minimum  $\Phi_\Omega$  is attained at a point  $\mathbf{x}_g \in \Omega$ ,

$$\int_{\Omega} e^{-\frac{\phi(\mathbf{x})}{D}} d\mathbf{x} \approx \frac{(\pi D)^{3/2}}{\sqrt{\det [H_{\Phi}(\mathbf{x}_g)]}} e^{-\frac{\Phi_\Omega}{D}}. \quad (74)$$

We conclude this section by indicating that the formulas presented above can be used to estimate the probability and the mean time for a stochastic viral particle to reach a nuclear pore inside the nucleus.

### 4.3 Effect of changing the window coverage on the escape time

For a large windows  $n \gg 1$ , distributed over a small surface  $S_a$  of a domain  $\Omega$ , the leading order term of the narrow escape time for a Brownian particle to one of the small window was derived using electrostatic [20]

$$\langle \tau \rangle_{ES} = \frac{|\Omega|}{D} \left( \frac{1}{C_{S_a}} + \frac{f(\sigma)}{4n\epsilon} \right), \quad (75)$$

where  $|\Omega|$  is the volume,  $C_{S_a}$  is the capacity of the surface  $\partial S_a$  where absorbing holes are distributed, and

$$\sigma = \frac{N\pi\epsilon^2}{|\partial S_a|} \quad (76)$$

is the fraction of  $S_a$  covered by the absorbing holes. When the surface  $S_a$  is a sphere of radius  $a$ , then  $C_{S_a} = 4\pi a$ , and the MFPT is given by

$$\langle \tau \rangle_{ES} = \frac{|\Omega|}{D} \left( \frac{1}{4\pi a} + \frac{f(\sigma)}{4n\epsilon} \right). \quad (77)$$

In general, the function  $f(\sigma)$  is unknown, but is given to leading order by  $f(\sigma) = 1$  [3]. Here, for a Brownian particle (no drift and no killing measure), the MFPT (eq. 66) reduces to

$$\langle \tau \rangle_{\Phi=0, k=0} \approx \frac{|\Omega|}{D} \left( \frac{1}{4\pi a} + \frac{1}{4n\epsilon} \left( 1 - \frac{n\epsilon}{\pi a} \left( 2\alpha_0 - \alpha_0^2 \log(\alpha_0) + \frac{1}{n} \log \left( \frac{\epsilon}{a} \right) \right) \right) \right) \quad (78)$$

Thus, we identify here the function

$$f(\sigma) = 1 - 8\frac{\sigma}{\pi} + \frac{\epsilon}{a\pi} (1 - 4\sigma) \log \left( \frac{\epsilon}{a} \right) + o \left( \frac{\epsilon}{a} \right) \quad (79)$$

when non-overlapping absorbing holes are randomly distributed and

$$f(\sigma) = 1 - 4\frac{\sqrt{\sigma}}{\pi} + \frac{\epsilon}{a\pi} \log(\sqrt{\sigma}) + o \left( \frac{\epsilon}{a} \right) \quad (80)$$

when absorbing holes are distributed homogeneously.

We end this section with two remarks. First, for  $\sigma \ll 1$ ,  $8\frac{\sigma}{\pi} < 4\frac{\sqrt{\sigma}}{\pi}$ , the MFPT of a single particle to an absorbing hole is higher for randomly distributed holes compared to homogeneously distributed holes. Second, formulas 79 and 80 derived here by accounting for two window coverage predict MFPT formula different than previously reported based on an effective medium treatment ( $f(\sigma) = 1 - \sigma$  [26]) or interpolated from Brownian simulations ( $f(\sigma) = \frac{1 - \sigma}{1 + 3.8\sigma^{1.25}}$  [2]). This difference may arise from the differences in the window arrangements.

## 5 Comparison of asymptotic formula with respect to Brownian simulations

For a ball of radius  $R$  with a centered sphere  $S_a$  (radius  $a$ ) uniformly covered by  $n$  small absorbing pores (radius  $\epsilon$ ) (Fig. 1 right). Stochastic particles are reflected on the external membrane  $r = R$  and on  $r = a$  except on all windows  $\partial N_a = \bigcup_{i=1}^n \partial \Omega_i$ , centered at random locations  $(\mathbf{x}_i)_{i=1}^n$ . We use a constant radial drift  $B$  directed toward the nucleus (with a potential  $\Phi(r) = -Br$ ). We consider a constant killing rate  $k(\mathbf{x}) = k_0$  and consequently, using function

$$G(D, B, a) = e^{-\frac{Ba}{D}} \left( \frac{D}{B} a^2 + 2 \left( \frac{D}{B} \right)^2 a + 2 \left( \frac{D}{B} \right)^3 \right) \quad (81)$$

expressions (69-70) simplify to

$$\langle P \rangle = \frac{e^{-\frac{Ba}{D}}}{\langle \tau \rangle_{\Phi=0, k=0} (G(D, B, a) - G(D, B, R)) k + e^{-\frac{Ba}{D}}}, \quad (82)$$

and

$$\langle \tau \rangle = \frac{\langle \tau \rangle_{\Phi=0, k=0} (G(D, B, a) - G(D, B, R))}{\langle \tau \rangle_{\Phi=0, k=0} (G(D, B, a) - G(D, B, R)) k + e^{-\frac{Ba}{D}}}. \quad (83)$$

In Fig. 2, we show how these expressions compare to stochastic simulations for an increasing number of holes while maintaining constant the ratio  $\sigma = \frac{n\pi\epsilon^2}{4\pi a^2}$  of the nucleus surface covered by the absorbing windows to the value  $\sigma = 2\%$ . This number was calibrated by using a surface covered by 2,000 pores of 25nm diameter on the nucleus of a chinese hamster ovary cell [17]). The parameters are summarized in table 1.

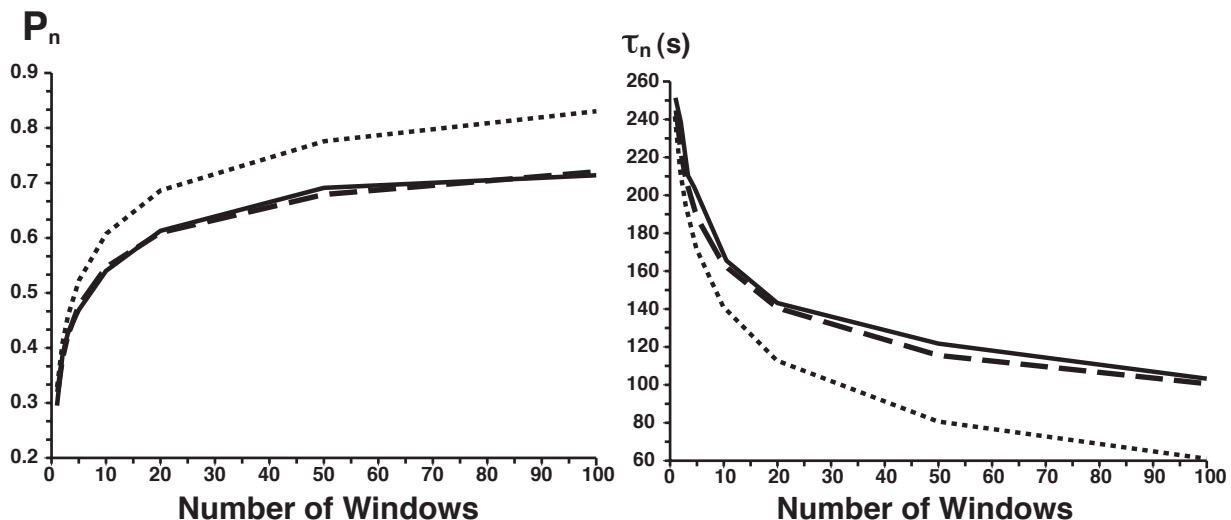


Figure 2: **Probability  $P_n$  (left) and conditional MFPT  $\tau_n$  (right).** Asymptotics formula 82 and 83 (dashed line) are compared to stochastic simulations (solid line) for an increasing number of absorbing windows, while the ratio  $\sigma = \frac{n\pi\epsilon^2}{4\pi a^2}$  of the absorbing to the total surface is kept constant  $\sigma = 2\%$  [17]. The asymptotics formula 6 that do not account for the window interactions is presented to visualize the improvement of the new formula (dotted line). 1000 stochastic trajectories are simulated. Parameters are summarized in table 1.

## 6 Conclusion

Intermittent dynamics with alternative periods of free diffusion and directed motion along MTs characterizes a large class of cellular transports. When the intermittent particle can be degraded through the ubiquitin-proteasome machinery or trapped in the crowded cytoplasm, we derived here improved asymptotics formula for the probability  $P_n$  and the mean time  $\tau_n$  to reach a small absorbing target among  $n$ . These formula accounts for the geometrical interactions between the windows. When the targets co-localize on a small domain  $S_a$ , asymptotics of  $P_n$  and  $\tau_n$  are obtained in the limit  $\frac{|S_a|}{|\Omega|} \ll 1$ . Applied to DNA viruses that have to reach a small nuclear pore among the 2,000, these formulas provide estimates for the arrival time to the nucleus. We confirmed here the validity of asymptotics formula 82-83) for the probability  $P_n$  and the mean time  $\tau_n$  respectively using Brownian simulations. We note that contrary to the classical narrow escape asymptotic where the leader order term contains most of the geometry, here the  $O(1)$ -term accounts for the interactions between windows. For example, where there are 100 windows, the asymptotic formula of the conditioned MFPT gives  $\tau_n \approx 2min$ , similar to simulation results, but is twice the one derived in [10], for which  $\tau_n \approx 1min..$



Parameter	Description	Value
$D$	Diffusion constant of the virus	$D = 1.3\mu m^2 s^{-1}$ (Observed for the Associated-Adeno-Virus [22])
$B$	Drift	$B = 0.2\mu m s^{-1}$ [13]
$\sigma$	% of the nuclear surface covered by $n$ nuclear pores	$\sigma = 2\%$ [17]
$k$	Degradation rate	$k = 1/360s^{-1}$ (10 times the rate observed for gene vectors [16])
$R$	Radius of the cell	$R = 15\mu m$ (Chinese hamster ovary cell)
$a$	Radius of the nucleus	$a = 5\mu m$ [17]

Table 1: Numerical parameters used for Brownian simulations

## 7 Appendix

We derive in this appendix the asymptotic of the Neumann's function  $\mathcal{N}(\mathbf{x}_i, \mathbf{x}_j)$  for two absorbing patches localized on the surface of a small ball of radius  $a$ . In that case, expansion of eq. 31 is not sufficient and the parameter  $a$  should be now accounted for.

Indeed, the log-term  $\frac{-1}{4\pi a D} \log\left(\frac{1}{|\mathbf{x}_i - \mathbf{x}_j|}\right)$  can be much larger than the leading order term  $\frac{1}{2\pi D |\mathbf{x}_i - \mathbf{x}_j|}$  when  $|\mathbf{x}_i - \mathbf{x}_j| \approx a$ , for  $a \ll |\Omega|^{\frac{1}{3}}$ . Consequently, we shall re-examine the log-term expansion. For  $\mathbf{x}$  and  $\mathbf{x}_0$  in the neighborhood of the sphere  $S_a$ , we expand the Neumann function  $\mathcal{N}(\mathbf{x}, \mathbf{x}_0)$  as

$$\mathcal{N}(\mathbf{x}, \mathbf{x}_0) = \tilde{\mathcal{N}}(\mathbf{x}, \mathbf{x}_0) + O(1), \quad (84)$$

where  $\tilde{\mathcal{N}}(\mathbf{x}, \mathbf{x}_0)$  is solution of with  $D = 1$ ,

$$\begin{aligned} \Delta \tilde{\mathcal{N}}(\mathbf{x}, \mathbf{x}_0) &= -\delta(\mathbf{x} - \mathbf{x}_0) \text{ for } \mathbf{x} \in \mathbb{R}^3 \\ \frac{\partial \tilde{\mathcal{N}}}{\partial n}(\mathbf{x}, \mathbf{x}_0) &= 0 \text{ for } \mathbf{x} \in S_a. \end{aligned} \quad (85)$$

To compute the log-term, we first decompose  $\tilde{\mathcal{N}}(\mathbf{x}, \mathbf{x}_0) = \frac{1}{4\pi|\mathbf{x} - \mathbf{x}_0|} + \Phi(\mathbf{x}, \mathbf{x}_0)$  where  $\Phi$  is solution of the system:

$$\begin{aligned} \Delta \Phi(\mathbf{x}, \mathbf{x}_0) &= 0, \text{ for } \mathbf{x} \in \mathbb{R}^3 \\ \frac{\partial \Phi}{\partial n}(\mathbf{x}, \mathbf{x}_0) &= -\frac{\partial}{\partial n} \left( \frac{1}{4\pi|\mathbf{x} - \mathbf{x}_0|} \right), \text{ for } \mathbf{x} \in S_a. \end{aligned} \quad (86)$$

To solve eq. 86, we choose a coordinate system so that the source point  $\mathbf{x} = \mathbf{x}_0$  is on the positive  $z$  axis. Since  $a\Phi = 0$  and  $\Phi$  is axisymmetric, then  $\Phi$  has the series expansion

$$\Phi(\mathbf{x}, \mathbf{x}_0) = \sum_{n=0}^{\infty} b_n(|\mathbf{x}_0|) \frac{P_n(\cos(\theta))}{|\mathbf{x}|^{n+1}}, \quad (87)$$

where  $P_n$  are the Legendre polynomials of integer  $n$ ,  $\theta$  is the angle between  $\mathbf{x}$  and the north pole and  $b_n(|\mathbf{x}_0|)$  are coefficients, determined from boundary condition 86.

For  $\mathbf{x} \in S_a$  and  $\rho = |\mathbf{x}|$ ,

$$\frac{\partial \Phi}{\partial n}(\mathbf{x}, \mathbf{x}_0) = \frac{\partial \Phi}{\partial \rho}(\rho = a) = - \sum_{n=0}^{\infty} \frac{(n+1) b_n(|\mathbf{x}_0|)}{a^{n+2}} P_n(\cos(\theta)). \quad (88)$$

On the other hand, for  $|\mathbf{x}| < |\mathbf{x}_0|$  we have the expansion

$$\frac{1}{4\pi|\mathbf{x} - \mathbf{x}_0|} = \frac{1}{4\pi} \sum_{n=0}^{\infty} \frac{|\mathbf{x}|^n}{|\mathbf{x}_0|^{n+1}} P_n(\cos(\theta)), \quad (89)$$

which leads to the boundary condition:

$$- \frac{\partial}{\partial \rho} \left( \frac{1}{4\pi|\mathbf{x} - \mathbf{x}_0|} \right) (\rho = a) = - \frac{1}{4\pi} \sum_{n=0}^{\infty} \frac{na^{n-1}}{|\mathbf{x}_0|^{n+1}} P_n(\cos(\theta)). \quad (90)$$

Injecting relation 88-90) into the boundary condition 86, we obtain that for all  $n \geq 0$ :

$$b_n(|\mathbf{x}_0|) = \frac{1}{4\pi} \frac{na^{2n+1}}{(n+1)|\mathbf{x}_0|^{n+1}}. \quad (91)$$

The Neumann function  $\tilde{\mathcal{N}}(\mathbf{x}, \mathbf{x}_0)$  is then given by:

$$\tilde{\mathcal{N}}(\mathbf{x}, \mathbf{x}_0) = \frac{1}{4\pi|\mathbf{x} - \mathbf{x}_0|} + \frac{1}{4\pi} \sum_{n=0}^{\infty} \frac{na^{2n+1}}{(n+1)|\mathbf{x}|^{n+1}|\mathbf{x}_0|^{n+1}} P_n(\cos(\theta)), \quad (92)$$

that we rewrite

$$\tilde{\mathcal{N}}(\mathbf{x}, \mathbf{x}_0) = \frac{1}{4\pi|\mathbf{x} - \mathbf{x}_0|} + \frac{1}{4\pi} \sum_{n=0}^{\infty} \left( \frac{a^{2n+1}}{|\mathbf{x}|^{n+1}|\mathbf{x}_0|^{n+1}} - \frac{a^{2n+1}}{(n+1)|\mathbf{x}|^{n+1}|\mathbf{x}_0|^{n+1}} \right) P_n(\cos(\theta)). \quad (93)$$

Using expansion 89), we have for the first term of 93

$$\frac{1}{4\pi} \sum_{n=0}^{\infty} \frac{a^{2n+1}}{|\mathbf{x}|^{n+1}|\mathbf{x}_0|^{n+1}} P_n(\cos(\theta)) = \frac{a}{4\pi|\mathbf{x}_0| \left| x - \frac{a^2 \mathbf{x}_0}{|\mathbf{x}_0|^2} \right|} \quad (94)$$

To compute the second term  $I(\rho) = - \sum_{n=0}^{\infty} \frac{a^{2n+1}}{(n+1)\rho^{n+1}|\mathbf{x}_0|^{n+1}} P_n(\cos(\theta))$ , we note that

$$I'(\rho) = \sum_{n=0}^{\infty} \frac{a^{2n+1}}{\rho^{n+2}|\mathbf{x}_0|^{n+1}} P_n(\cos(\theta)) = \frac{a}{\rho|\mathbf{x}_0| \left| x - \frac{a^2 \mathbf{x}_0}{|\mathbf{x}_0|^2} \right|}, \quad (95)$$

that is

$$I'(\rho) = \frac{1}{\rho a \left(1 + \frac{|\mathbf{x}_0|^2 \rho^2}{a^4} - 2 \frac{|\mathbf{x}_0| \rho}{a^2} \cos(\theta)\right)^{\frac{1}{2}}}. \quad (96)$$

Because  $\lim_{\rho \rightarrow \infty} l(\rho) = 0$ , we have:

$$l(\rho) = - \int_{\rho}^{\infty} I'(s) ds = - \int_{\rho}^{\infty} \frac{ds}{sa \left(1 + \frac{|\mathbf{x}_0|^2 s^2}{a^4} - 2 \frac{|\mathbf{x}_0| s}{a^2} \cos(\theta)\right)^{\frac{1}{2}}}. \quad (97)$$

Thus,

$$l(\rho) = \frac{1}{a} \log \left( \frac{\frac{|\mathbf{x}_0| \rho}{a^2} (1 - \cos(\theta))}{1 - \frac{|\mathbf{x}_0| \rho}{a^2} \cos(\theta) + \left(1 + \left(\frac{|\mathbf{x}_0| \rho}{a^2}\right)^2 - 2 \frac{|\mathbf{x}_0| \rho}{a^2} \cos(\theta)\right)^{\frac{1}{2}}} \right). \quad (98)$$

Finally, we obtain the expression of the Neumann function  $\tilde{\mathcal{N}}(\mathbf{x}, \mathbf{x}_0)$  and the exact dependency with the inner ball radius:

$$\begin{aligned} \tilde{\mathcal{N}}(\mathbf{x}, \mathbf{x}_0) &= \frac{1}{4\pi |\mathbf{x} - \mathbf{x}_0|} + \frac{a}{4\pi D |\mathbf{x}_0| |x - \frac{a^2 \mathbf{x}_0}{|\mathbf{x}_0|^2}|} \\ &+ \frac{1}{4\pi a} \log \left( \frac{\frac{|\mathbf{x}_0| |\mathbf{x}|}{a^2} (1 - \cos(\theta))}{1 - \frac{|\mathbf{x}_0| |\mathbf{x}|}{a^2} \cos(\theta) + \left(1 + \left(\frac{|\mathbf{x}_0| |\mathbf{x}|}{a^2}\right)^2 - 2 \frac{|\mathbf{x}_0| |\mathbf{x}|}{a^2} \cos(\theta)\right)^{\frac{1}{2}}} \right) \end{aligned} \quad (99)$$

When  $\mathbf{x}$  and  $\mathbf{x}_0$  are on the sphere  $S_a$ ,  $|\mathbf{x}_0| = |\mathbf{x}| = a$ , we have

$$\tilde{\mathcal{N}}(\mathbf{x}, \mathbf{x}_0) = \frac{1}{2\pi |\mathbf{x} - \mathbf{x}_0|} + \frac{1}{4\pi a} \log \left( \frac{|\mathbf{x} - \mathbf{x}_0|}{2a + |\mathbf{x} - \mathbf{x}_0|} \right). \quad (100)$$

**Acknowledgments:** T.L. is supported by a FRM post-doctoral fellowship and a grant from Philippe Foundation. D. H. research is supported by a Marie-Curie fellowship.

## References

- [1] Arhel, N., Genovesio, A., Kim, K.A., Miko, S., Perret, E., Olivo-Marin, J.C., Shorte, S., Charneau, P.: Quantitative four-dimensional tracking of cytoplasmic and nuclear hiv-1 complexes. *Nat Methods* **3**(10), 817–24 (2006). DOI 10.1038/nmeth928

- [2] Berezhkovskii, A.M., Makhnovskii, Y.A., Monine, M.I., Zitserman, V.Y., Shvartsman, S.Y.: Boundary homogenization for trapping by patchy surfaces. *J Chem Phys* **121**(22), 11,390–4 (2004). DOI 10.1063/1.1814351
- [3] Berg, H.C., Purcell, E.M.: Physics of chemoreception. *Biophys J* **20**(2), 193–219 (1977). DOI 10.1016/S0006-3495(77)85544-6
- [4] Cheviakov, A.F., Ward, M., Straube, R.: An asymptotic analysis of the mean first passage time for narrow escape problems: Part ii: The sphere. *SIAM Multiscale Modeling and Simulation* **8**(3), 836–870 (2010)
- [5] Cheviakov, A.F., Zawada, D.: Narrow-escape problem for the unit sphere: homogenization limit, optimal arrangements of large numbers of traps, and the n(2) conjecture. *Phys Rev E Stat Nonlin Soft Matter Phys* **87**(4), 042,118 (2013). DOI 10.1103/PhysRevE.87.042118
- [6] Coombs, D., Straube, R., Ward, M.: Diffusion on a sphere with localized traps: Mean first passage time, eigenvalue asymptotics, and fekte points. *Siam Journal On Applied Mathematics* **70**(1), 302–332 (2009)
- [7] Dauty, E., Verkman, A.S.: Actin cytoskeleton as the principal determinant of size-dependent dna mobility in cytoplasm: a new barrier for non-viral gene delivery. *J Biol Chem* **280**(9), 7823–8 (2005). DOI 10.1074/jbc.M412374200
- [8] Dynes, J.L., Steward, O.: Dynamics of bidirectional transport of arc mrna in neuronal dendrites. *J Comp Neurol* **500**(3), 433–47 (2007). DOI 10.1002/cne.21189
- [9] Greber, U.F., Way, M.: A superhighway to virus infection. *Cell* **124**(4), 741–54 (2006). DOI 10.1016/j.cell.2006.02.018
- [10] Holcman, D.: Modeling dna and virus trafficking in the cell cytoplasm. *Journal of Statistical Physics* **127**(3), 471–494 (2007)
- [11] Holcman, D., Marchewka, A., Schuss, Z.: Survival probability of diffusion with trapping in cellular neurobiology. *Phys Rev E Stat Nonlin Soft Matter Phys* **72**(3 Pt 1), 031,910 (2005). DOI 10.1103/PhysRevE.72.031910
- [12] Holcman, D., Schuss, Z.: Diffusion through a cluster of small windows and flux regulation in microdomains. *Physics Letters A* **372**(21), 3768–3772 (2008)
- [13] Lagache, T., Dauty, E., Holcman, D.: Quantitative analysis of virus and plasmid trafficking in cells. *Phys Rev E Stat Nonlin Soft Matter Phys* **79**(1 Pt 1), 011,921 (2009). DOI 10.1103/PhysRevE.79.011921
- [14] Lagache, T., Holcman, D.: Effective motion of a virus trafficking inside a biological cell. *Siam Journal On Applied Mathematics* **68**(4), 1146–1167 (2008)

- [15] Lagache, T., Holcman, D.: Quantifying intermittent transport in cell cytoplasm. *Phys Rev E Stat Nonlin Soft Matter Phys* **77**(3 Pt 1), 030,901 (2008). DOI 10.1103/PhysRevE.77.030901
- [16] Lechardeur, D., Sohn, K.J., Haardt, M., Joshi, P.B., Monck, M., Graham, R.W., Beatty, B., Squire, J., O’Brodivich, H., Lukacs, G.L.: Metabolic instability of plasmid dna in the cytosol: a potential barrier to gene transfer. *Gene Ther* **6**(4), 482–97 (1999). DOI 10.1038/sj.gt.3300867
- [17] Maul, G.G., Deaven, L.: Quantitative determination of nuclear pore complexes in cycling cells with differing dna content. *J Cell Biol* **73**(3), 748–60 (1977)
- [18] Medalia, O., Weber, I., Frangakis, A.S., Nicastro, D., Gerisch, G., Baumeister, W.: Macromolecular architecture in eukaryotic cells visualized by cryoelectron tomography. *Science* **298**(5596), 1209–13 (2002). DOI 10.1126/science.1076184
- [19] Pillay, S., Ward, M., Pierce, A., Kolokolnikov, T.: An asymptotic analysis of the mean first passage time for narrow escape problems: Part i: Two-dimensional domains. *SIAM Multiscale Modeling and Simulation* **8**(3), 803–835 (2010)
- [20] Reingruber, J., Abad, E., Holcman, D.: Narrow escape time to a structured target located on the boundary of a microdomain. *J Chem Phys* **130**(9), 094,909 (2009). DOI 10.1063/1.3081633
- [21] Schuss, Z., Holcman, D.: Diffusion escape through a cluster of small absorbing windows. *Journal of Physics A: Mathematical and Theoretical* **41**(15), 155,001 (2008)
- [22] Seisenberger, G., Ried, M.U., Endress, T., Büning, H., Hallek, M., Bräuchle, C.: Real-time single-molecule imaging of the infection pathway of an adeno-associated virus. *Science* **294**(5548), 1929–32 (2001). DOI 10.1126/science.1064103
- [23] Singer, A., Schuss, Z., Holcman, D.: Narrow escape and leakage of brownian particles. *Phys Rev E Stat Nonlin Soft Matter Phys* **78**(5 Pt 1), 051,111 (2008). DOI 10.1103/PhysRevE.78.051111
- [24] Sodeik, B.: Mechanisms of viral transport in the cytoplasm. *Trends Microbiol* **8**(10), 465–72 (2000)
- [25] Zuber, G., Dauty, E., Nothisen, M., Belguise, P., Behr, J.P.: Towards synthetic viruses. *Adv Drug Deliv Rev* **52**(3), 245–53 (2001)
- [26] Zwanzig, R.: Diffusion-controlled ligand binding to spheres partially covered by receptors: an effective medium treatment. *Proc Natl Acad Sci U S A* **87**(15), 5856–7 (1990)